

---

# Orthogonal Gradient Descent Improves Neural Calibration

---

C. Evans Hedges  
University of Denver  
evans.hedges@du.edu

## Abstract

We provide evidence that orthogonalizing gradients during training improves model calibration without sacrificing accuracy. On CIFAR-10 with 10% labeled data,  $\perp$ Grad matches SGD in accuracy but yields consistently improved calibration metrics such as lower test loss, reduced softmax overconfidence, and higher predictive entropy. These benefits persist under input corruption (CIFAR-10C) and extended training, where  $\perp$ Grad models degrade more gracefully than SGD-trained counterparts.  $\perp$ Grad is optimizer-agnostic, incurs minimal overhead, and works well with post-hoc calibration techniques like temperature scaling.

Theoretically, we prove convergence of a simplified version of  $\perp$ Grad under mild assumptions and characterize its stationary points in positive homogeneous networks:  $\perp$ Grad converges to solutions where further loss reduction requires confidence scaling rather than decision boundary improvement.

## 1 Introduction

Neural networks are increasingly deployed in settings where prediction confidence influences downstream decisions. In such contexts, model calibration—how well predicted probabilities reflect true correctness—is as critical as accuracy. Modern deep networks are often poorly calibrated, tending toward overconfidence even when incorrect.

Existing calibration approaches fall into two categories: intrinsic methods that alter training objectives, and post-hoc methods like temperature scaling. In this work, we investigate a third axis: modifying the optimization geometry. Specifically, we study orthogonal gradient descent ( $\perp$ Grad), which projects gradients to be orthogonal to layer weights during training.

We evaluate  $\perp$ Grad empirically on CIFAR-10 and CIFAR-10C using both ResNet18 and WideResNet-28-10, with a focus on the low-data regime. Our results show that  $\perp$ Grad consistently reduces test loss and various calibration metrics (including softmax confidence and expected calibration error) without impacting accuracy. These improvements persist under input corruption and extended training, and remain compatible with post-hoc calibration techniques. The method is simple to implement and optimizer-agnostic.

Theoretically, we prove convergence of a simplified  $\perp$ Grad variant and characterize its fixed points in positive homogeneous networks. These results suggest a mechanism by which  $\perp$ Grad prevents loss reduction via confidence scaling alone, encouraging decision-boundary improvements instead. Together, our findings show that geometry-aware optimization can enhance calibration.

## 2 Background

A classifier is said to be calibrated when the predicted confidence scores match the true likelihood of correctness. Informally, if a model assigns 70% confidence to a group of predictions, approximately

70% of those predictions should be correct. This property is important in settings where predictive uncertainty informs downstream decisions. Guo et al. introduced temperature scaling in [1] as a simple yet effective post-hoc calibration method, demonstrating that modern neural networks are often poorly calibrated despite high accuracy.

Calibration techniques can be grouped into intrinsic and post-hoc categories. Intrinsic methods aim to improve calibration during training, such as through loss function modifications [2, 3], data augmentation, or regularization strategies like mixup [5]. Post-hoc methods, by contrast, adjust the trained model’s outputs without altering its weights. These include temperature scaling, Platt scaling, and isotonic regression.

In [7], Wang et al. found empirically that many regularization techniques that lead to better model calibration were not as *calibratable* via post-hoc methods such as temperature scaling. This indicates that amenability to calibration is an important factor to consider when evaluating intrinsic calibration techniques. However, while effective, post-hoc methods rely on held-out validation data and cannot correct poor uncertainty estimation rooted in model internals.

Several prior works have explored the use of orthogonality to improve deep learning models. Wang et al. studied orthogonal convolutional filters in [8] to reduce feature redundancy, yielding improved generalization. Xie et al. [9] and Tuddenham et al. [6] explored enforcing orthogonality between gradients across layers, reporting training speedups. These methods primarily target stability or efficiency, rather than uncertainty estimation.

In contrast, we focus on orthogonal gradient descent,  $\perp$ Grad, where each gradient update is orthogonalized with respect to the current weight vector at the layer level. This is inspired by Prieto et al. [4], who introduced  $\perp$ Grad to accelerate grokking. Their method reprojects the layer-wise gradient to be orthogonal to the layer’s current weight vector and then renormalizes it to preserve the original gradient norm. A detailed description of  $\perp$ Grad can be found in [4] as well as the appendix of this paper. While their work focused on learning dynamics near instability, we apply  $\perp$ Grad in a new context: calibration. Specifically, we examine how this geometric constraint influences the model’s ability to estimate uncertainty under limited data and distribution shift.

To our knowledge, no prior work has directly studied the connection between orthogonal gradient updates and model calibration. Our work is the first to empirically investigate whether gradient orthogonalization can improve calibration metrics—such as expected calibration error (ECE) and predictive entropy—without harming accuracy.

### 3 Theoretical Analysis

To provide a basic theoretical grounding, we initially consider a simplified variant of  $\perp$ Grad where we do not renormalize the gradient after orthogonalization. For this variation, we prove the following result:

**Theorem 3.1.** *Suppose  $L : \mathbb{R}^n \rightarrow \mathbb{R}$  is bounded from below, differentiable, and  $\nabla L$  is Lipschitz with Lipschitz constant  $k$ . Then for any  $\eta \in (0, 1/k)$ , and any initialization  $x_0 \in \mathbb{R}^n$ ,  $\perp$ Grad (without gradient renormalization) will converge to some  $x^*$  satisfying:*

$$|\langle \nabla L(x^*), x^* \rangle| = \|x^*\| \cdot \|\nabla L(x^*)\|.$$

*In particular,  $\nabla L(x^*)$  is parallel to  $x^*$ .*

The proof of this theorem uses techniques that are standard for convergence results and details can be found in the appendix. For clarity we will discuss orthogonalization at the model level, however the argument extends naturally, with only notational or scaling-level modifications, to layer-level orthogonalization.

Notably, this means that  $\perp$ Grad will converge to solutions for which the only way to improve the loss is to scale the model weights and biases. As mentioned in [4], when the model is positive homogenous this corresponds to not changing the decision boundary, but instead only increasing the confidence of predicted classes. Thus,  $\perp$ Grad will converge to stationary points with respect to the decision boundary, and will not arbitrarily increase confidence to decrease loss.

While we cannot guarantee convergence for the renormalized variant, we show that if it converges, it must do so to a stationary point of the loss function. This may limit the benefits of the convergence

behavior available in the renormalized case. That being said, the fact that  $\perp$ Grad enforces orthogonal updates ensures that in positive homogenous networks, the updates do not simply inflate model confidence and instead aim to improve loss by altering the decision boundary. This explains why we may observe increasing softmax confidence and entropy without changes in accuracy in the case where gradients are not orthogonalized: the model becomes more confident in its decision boundary by scaling weights. This suggests that orthogonalizing gradients may prevent the model from naively scaling confidence without improving its decision boundary.

For the following empirical work we perform renormalization to align our techniques with those in [4].

## 4 CIFAR-10 Results

### 4.1 Training on CIFAR-10

Using 20 different seeds, we selected a random 10% of the training dataset, for a total of 500 images per class. For each seed, we trained a ResNet18 model (modified to fit the CIFAR-10 dataset) for 100 epochs with a learning rate of 0.01, momentum set to 0.9, and weight decay at  $5e - 4$ . We used a batch size of 64 and added random flips and crops for data augmentation. The base optimizer was pytorch’s SGD, which we compared to  $\perp$ Grad following the implementation in [4]. Note that this implementation includes gradient renormalization; while this variant does not enjoy the convergence guarantees we prove, we include it here for continuity with prior work and to isolate the effect of orthogonalization on calibration metrics. The average results across the 20 runs are shown in Table 1 and reliability diagrams can be found in the appendix.

	SGD	$\perp$ Grad	Effect Size	95% Confidence Interval	<i>p</i> value
Top1 Accuracy	75.18	<b>75.27</b>	-0.05	(-0.67, 0.57)	0.86
Top5 Accuracy	97.67	<b>97.81</b>	-0.35	(-0.97, 0.28)	0.28
Loss	1.26	<b>1.19</b>	0.64	(0.005, 1.28)	0.05
ECE	0.168	<b>0.161</b>	0.48	(-0.15, 1.11)	0.14
Brier Score	0.408	<b>0.400</b>	0.28	(-0.34, 0.91)	0.37
Entropy	0.208	<b>0.224</b>	-1.11	(-1.77, -0.44)	0.001
Max Softmax	0.920	<b>0.914</b>	1.06	(0.40, 1.72)	0.002
Max Logit	13.58	<b>13.03</b>	1.52	(0.82, 2.22)	$2.5 \times 10^{-5}$
Logit Variance	45.73	<b>42.30</b>	2.00	(1.25, 2.77)	$2 \times 10^{-7}$

Table 1: **CIFAR-10 test results across 20 seeds comparing SGD and  $\perp$ Grad.** Accuracy remains unchanged, but  $\perp$ Grad consistently improves loss, entropy, and softmax/logit statistics. These differences suggest improved calibration and reduced overconfidence under  $\perp$ Grad. Bold indicates better performance (higher accuracy, entropy; lower loss, ECE, etc.), regardless of statistical significance.

This experiment showed effectively no difference in the resulting models when it comes to Top1 and Top5 accuracy. However, there were consistent differences in a number of metrics that relate to model confidence.  $\perp$ Grad showed consistently lower test loss, higher entropy, and significantly more conservative logit/softmax output characteristics.

Additionally, while not statistically significant,  $\perp$ Grad showed improved ECE and Brier Score as well as better correlation between confidence and correctness (0.467) compared to SGD (0.445). These results suggest  $\perp$ Grad may encourage more uncertainty aware predictions, indicating better model calibration when compared to SGD.

While orthogonalization has been hypothesized to introduce implicit regularization by reducing weight norm growth, our experiments do not support this effect. The final weight vector norms did not differ significantly between the two optimization methods (79.69 for SGD compared to 79.72 for  $\perp$ Grad,  $p = 0.36$ ).

### 4.2 Temperature Scaling

Next, we evaluated the impact of temperature scaling on model calibration between the two optimizer choices. There was a significant difference ( $p = 0.003$ ) between optimal temperatures, with SGD

requiring higher temperature scaling ( $T = 2.80$ ) compared with  $\perp$ Grad ( $T = 2.66$ ). However, there was no difference between the temperature scaled ECE or Brier scores (see Table 2).

Optimizer	ECE		Brier Score	
	Before	After	Before	After
SGD	0.168	0.015	0.041	0.034
$\perp$ Grad	<b>0.161</b>	0.015	<b>0.040</b>	0.034

Table 2: **Expected Calibration Error (ECE) and Brier Score before and after temperature scaling on CIFAR-10.** Both optimizers benefit similarly from temperature scaling, but  $\perp$ Grad starts with slightly better raw calibration. This shows that  $\perp$ Grad is compatible with post-hoc calibration techniques, preserving gains after temperature correction. Bold indicates better performance, regardless of statistical significance.

Notably this means that, unlike the results in [7],  $\perp$ Grad appears to remain amenable to post-hoc calibration and is able to improve loss and entropy by instead optimizing the decision boundary without allowing for naive scaling of outputs. Additionally, the fact that  $\perp$ Grad required a significantly lower temperature for calibration further indicates that  $\perp$ Grad converges to better calibrated models without sacrificing accuracy.

### 4.3 CIFAR-10C Evaluation

Finally, we turn to examining how the resulting models behaved under input corruption using the CIFAR-10C dataset. We found that  $\perp$ Grad maintained calibration and loss improvements across corruption types and severity levels. We observed similar results to the clean experiment, with negligible differences between SGD and  $\perp$ Grad in accuracy metrics, but the effects on loss, entropy, max softmax/logit values, and logit variance persisted (although diminished in statistical significance).

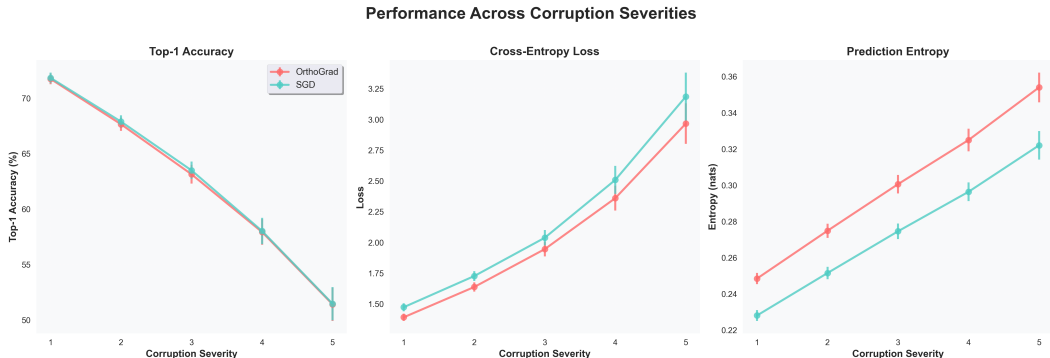


Figure 1: **Comparative trends across CIFAR-10C corruption levels.**  $\perp$ Grad consistently shows better loss and predictive entropy across corruption levels without sacrificing accuracy, indicating improved robustness under input noise.

In all, it appears that orthogonalizing gradients had no meaningful impact on accuracy, yet it improved the model’s calibration by decreasing loss and confidence and increasing entropy.

## 5 Additional Empirical Results

### 5.1 Extended Training Results

In order to investigate how calibration and robustness evolve under extreme overfitting, we deliberately extended training of ResNet18 to 1000 epochs, keeping all other hyperparameters constant. This serves as a stress test, revealing differences in optimizer behavior beyond the typical training horizon. Early stopping was not used, as our goal was to examine how  $\perp$ Grad shapes the minima found under prolonged training in a low-data regime. Due to computational constraints, we present results from a single seed and statistical conclusions should not be drawn. While these results are consistent with

our short-run multi-seed findings, a full statistical treatment of long-horizon calibration behavior remains future work.

SGD achieved higher test accuracy (70.5%) compared to  $\perp$ Grad (65.8%). However,  $\perp$ Grad consistently outperformed SGD under corruption: from level 2 onward, it showed better loss and ECE, and from level 3 onward, better Top1 accuracy. This resulted in better overall average accuracy across CIFAR-10C (60.4%) compared with SGD (59.0%). Accuracy comparisons across corruption levels can be found in Figure 2 in the appendix.

Corruption Level	Accuracy (%)		Loss		ECE		Conf-Acc Corr.	
	SGD	$\perp$ Grad	SGD	$\perp$ Grad	SGD	$\perp$ Grad	SGD	$\perp$ Grad
1	<b>67</b>	64	<b>1.79</b>	1.91	<b>0.23</b>	0.24	<b>0.388</b>	0.382
2	63	63	2.02	<b>1.93</b>	0.26	<b>0.24</b>	0.366	<b>0.384</b>
3	59	<b>61</b>	2.62	<b>2.00</b>	0.29	<b>0.25</b>	0.347	<b>0.377</b>
4	55	<b>59</b>	2.53	<b>2.08</b>	0.32	<b>0.26</b>	0.329	<b>0.374</b>
5	51	<b>55</b>	2.88	<b>2.24</b>	0.36	<b>0.28</b>	0.301	<b>0.343</b>

Table 3: **Accuracy, loss, ECE, and confidence–accuracy correlation on CIFAR-10C across corruption levels (single seed, 1000 epochs).**  $\perp$ Grad degrades more gracefully under corruption, outperforming SGD from corruption level 3 onward. Calibration and loss are consistently better, even though clean accuracy is slightly lower. Results suggest robustness gains under overfitting conditions. Bold indicates better performance, regardless of statistical significance.

Interestingly, at corruption level 5 the overfit  $\perp$ Grad model outperformed not only the overfit SGD model, but also outperformed every seed of  $\perp$ Grad and SGD from the 100 epoch experiment. Future work exploring the statistical robustness of these preliminary results is required.

## 5.2 WideResNet-28-10

We additionally ran a 5 seed experiment using WideResNet-28-10. All other hyperparameters were kept the same as the original ResNet18 experiment in Section 4. The results further confirm the trend that  $\perp$ Grad improves calibration metrics without sacrificing model accuracy. Although not statistically significant ( $p = 0.10$ ),  $\perp$ Grad resulted in higher correlation between predictions and accuracy (0.44) compared with SGD (0.42). These results persisted over corruption as evaluated in CIFAR-10C. Reliability diagrams can be found in the Appendix.

	SGD	$\perp$ Grad	Effect Size	95% Confidence Interval	$p$ value
Top1 Accuracy	78.54	<b>79.00</b>	-0.35	(-1.60, 0.90)	0.59
Top5 Accuracy	<b>98.05</b>	97.84	0.50	(-0.76, 1.76)	0.44
Loss	1.05	<b>0.88</b>	2.56	(0.89, 4.24)	0.004
ECE	0.14	<b>0.12</b>	2.40	(0.77, 4.02)	0.015
Brier Score	0.35	<b>0.33</b>	0.86	(-0.43, 2.15)	0.21
Entropy	0.19	<b>0.25</b>	-4.18	(-6.40, -1.97)	$2 \times 10^{-4}$
Max Softmax	0.92	<b>0.91</b>	2.91	(1.13, 4.69)	0.002
Max Logit	12.11	<b>8.68</b>	11.20	(6.14, 16.27)	$3 \times 10^{-6}$
Logit Variance	31.37	<b>13.83</b>	15.45	(8.57, 22.34)	$6 \times 10^{-6}$

Table 4: **CIFAR-10 WideResNet-28-10 test results across 5 seeds comparing SGD and  $\perp$ Grad.** Accuracy remains unchanged, but  $\perp$ Grad consistently improves loss, entropy, and softmax/logit statistics. These differences suggest improved calibration and reduced overconfidence under  $\perp$ Grad. Bold indicates better performance, regardless of statistical significance.

## 6 Discussion

The primary contribution of this work is empirical: a demonstration that gradient orthogonalization via  $\perp$ Grad leads to improved model calibration without sacrificing accuracy, particularly in low-data and distribution-shifted settings. These results are consistent across seeds and metrics, and persist under both moderate corruption and long-horizon training, where calibration often deteriorates. The

method is optimizer-agnostic and simple to implement, making it a low-cost intervention for settings where confidence reliability matters.

Despite these strengths, several limitations remain. First, our analysis is confined to CIFAR-10 and CIFAR-10C. Whether the observed calibration improvements generalize to larger-scale datasets, different architectures, or non-vision domains remains an open question. Additionally, while the extended training results provide suggestive evidence of robustness, they are based on a single seed and should not be over-interpreted.

Additionally, our results suggest that  $\perp$ Grad responds well to temperature scaling, mitigating concerns that arise from [7] where it was observed that although some regularized models appear well-calibrated, they respond poorly to post-hoc methods like temperature scaling. Beyond temperature scaling, the interaction between  $\perp$ Grad and regularization strategies like dropout, label smoothing, or mixup remains to be explored.

From a theoretical standpoint, we offer a convergence result for a non-renormalized variant of  $\perp$ Grad, and provide a characterization of stable points that links gradient geometry to softmax behavior for a large class of neural networks. These stable points show favorable behavior, in that locally loss cannot be improved further by changing the decision boundary.

Unfortunately the proof technique used to show convergence in non-renormalized  $\perp$ Grad cannot be used directly for convergence in the renormalized variant used in this study, and we suspect that convergence cannot be guaranteed in this case. While renormalization was included for consistency with [4], we plan to directly evaluate the non-renormalized variant of  $\perp$ Grad in future work to assess whether its theoretical advantages translate to improved results in practice.

In summary, we show that orthogonalizing gradients during training improves neural network calibration without sacrificing accuracy. Our experiments demonstrate that  $\perp$ Grad resists overconfident estimates under limited data, distribution shift, and extended training. The method is simple to implement, optimizer-agnostic, and compatible with post-hoc calibration. While further validation on larger and more diverse datasets is needed, our findings suggest that geometric constraints on gradient updates offer a promising direction for improving model reliability.

## References

- [1] Chuan Guo, Geoff Pleiss, Yu Sun, and Kilian Q Weinberger. On calibration of modern neural networks. In *International conference on machine learning*, pages 1321–1330. PMLR, 2017.
- [2] Aviral Kumar, Sunita Sarawagi, and Ujjwal Jain. Trainable calibration measures for neural networks from kernel mean embeddings. In *International Conference on Machine Learning*, pages 2805–2814. PMLR, 2018.
- [3] Jishnu Mukhoti, Viveka Kulharia, Amartya Sanyal, Stuart Golodetz, Philip Torr, and Puneet Dokania. Calibrating deep neural networks using focal loss. *Advances in neural information processing systems*, 33:15288–15299, 2020.
- [4] Lucas Prieto, Melih Barsbey, Pedro AM Mediano, and Tolga Birdal. Grokking at the edge of numerical stability. *arXiv preprint arXiv:2501.04697*, 2025.
- [5] Sunil Thulasidasan, Gopinath Chennupati, Jeff A Bilmes, Tanmoy Bhattacharya, and Sarah Michalak. On mixup training: Improved calibration and predictive uncertainty for deep neural networks. *Advances in neural information processing systems*, 32, 2019.
- [6] Mark Tuddenham, Adam Prügél-Bennett, and Jonathan Hare. Orthogonalising gradients to speed up neural network optimisation. *arXiv preprint arXiv:2202.07052*, 2022.
- [7] Deng-Bao Wang, Lei Feng, and Min-Ling Zhang. Rethinking calibration of deep neural networks: Do not be afraid of overconfidence. *Advances in Neural Information Processing Systems*, 34:11809–11820, 2021.
- [8] Jiayun Wang, Yubei Chen, Rudransis Chakraborty, and Stella X Yu. Orthogonal convolutional neural networks. In *Proceedings of the IEEE/CVF conference on computer vision and pattern recognition*, pages 11505–11515, 2020.

- [9] Di Xie, Jiang Xiong, and Shiliang Pu. All you need is beyond a good init: Exploring better solution for training extremely deep convolutional neural networks with orthonormality and modulation. In Proceedings of the IEEE Conference on Computer Vision and Pattern Recognition, pages 6176–6185, 2017.

## 7 Appendix

The appendix is organized as follows. First we begin with a theoretical exploration of  $\perp$ Grad with renormalization as used in this study and in [4]. We then prove Theorem 3.1, showing that in the non-renormalized case  $\perp$ Grad is guaranteed to converge under standard assumptions. We then discuss the stable points for  $\perp$ Grad, showing that in the case of positive homogenous classification networks they correspond with stationary points with respect to the decision boundary.

### 7.1 $\perp$ Grad with Renormalization

First we formally define the  $\perp$ Grad algorithm for continuous loss functions on  $\mathbb{R}^n$ . There are two important variations. First, we define the variation that is used in [4], as well as used for the empirical results in this paper:  $\perp$ Grad with renormalization.

**Definition 7.1.** *For a differentiable loss function  $L : \mathbb{R}^n \rightarrow \mathbb{R}$ , learning rate  $\eta > 0$ , numerical stability constant  $\epsilon > 0$ , we define the  $\perp$ Grad update procedure as follows:*

1. Begin with  $x \in \mathbb{R}^n$ ,
2. Next let  $g = \nabla L(x) - \frac{\langle \nabla L(x), x \rangle}{\|x\|^2} x$ . This is the orthogonalized gradient.
3. If  $\|g\| = 0$ , we do not perform an update and return  $x$ . Otherwise we continue.
4. We now scale the gradient according to  $\alpha \in [0, 1]$ :

$$\hat{g} = \left( \frac{\|\nabla L(x)\|}{\|g\| + \epsilon} \right) g.$$

5. Finally, we update  $x' = x - \eta \hat{g}$ .

Note here that we re-normalize the orthogonalized gradient to have the same magnitude as the original gradient (with a slight modification for numerical stability purposes). Unfortunately this renormalization leads to slightly less desirable theoretical properties. In particular, if  $\perp$ Grad with renormalization converges, it converges to a stationary point for  $L$ . Note that this does not imply that  $\perp$ Grad with renormalization will converge, and in fact with a fixed learning rate we suspect that in many cases it will not converge, but we leave a deeper discussion of this potential lack of convergence to future work.

**Lemma 7.2.** *If  $\perp$ Grad with renormalization converges along the descent pathway  $(x_k)_{k \in \mathbb{N}}$ , then either  $\langle \nabla L(x_k), x_k \rangle = \|x_k\| \cdot \|\nabla L(x_k)\|$  for some  $k \in \mathbb{N}$  at which point the  $\perp$ Grad trajectory stabilizes, or  $\|\nabla L(x_k)\| \rightarrow 0$ .*

*Proof.* First suppose  $\perp$ Grad converges along the descent pathway  $(x_k)_{k \in \mathbb{N}}$ . If we have  $\langle \nabla L(x_k), x_k \rangle = \|x_k\| \cdot \|\nabla L(x_k)\|$  for some  $k$ , it is easy to see that the  $\perp$ Grad trajectory stabilizes. We now assume that  $\langle \nabla L(x_k), x_k \rangle \neq 0$  for all  $k \in \mathbb{N}$ . For each  $k \in \mathbb{N}$ , let  $v_k, \hat{g}_k$  be as in the definition of  $\perp$ Grad. Since  $(x_k)$  converges, we have

$$\|\hat{g}_k\| = \frac{\|\nabla L(x_k)\| \cdot \|v_k\|}{\|v_k\| + \epsilon} = \frac{\|\nabla L(x_k)\|}{1 + \frac{\epsilon}{\|v_k\|}} \rightarrow 0.$$

Suppose for a contradiction that  $\limsup \|\nabla L(x_k)\| = c > 0$ . By passing to a subsequence we can assume without loss of generality that  $\lim \|\nabla L(x_k)\| = c$ . Since  $\|v_k\| \leq \|\nabla L(x_k)\|$  by definition, we know

$$\limsup 1 + \frac{\epsilon}{\|v_k\|} \geq 1 + \frac{\epsilon}{c},$$

and therefore

$$\liminf \frac{\|\nabla L(x_k)\|}{1 + \frac{\epsilon}{\|v_k\|}} \geq \frac{c}{1 + \frac{\epsilon}{c}} > 0.$$

This contradicts that  $\|\hat{g}_k\| \rightarrow 0$  and it must be the case that  $\|\nabla L(x_k)\| \rightarrow 0$ .  $\square$

Notably, this means that if the  $\perp$ Grad procedure outlined in [4] converges (nontrivially), it converges to a stationary point for  $L$ . Combined with the fact that we cannot guarantee convergence for the renormalized version of  $\perp$ Grad, this may mitigate some of the theoretically proposed benefits discussed in Section 3.

## 7.2 Proof of Theorem 3.1

Next we define the  $\perp$ Grad procedure without renormalization:

**Definition 7.3.** For a differentiable loss function  $L : \mathbb{R}^n \rightarrow \mathbb{R}$ , learning rate  $\eta > 0$ , we define the  $\perp$ Grad (without renormalization) update procedure as follows:

1. Begin with  $x \in \mathbb{R}^n$ ,
2. Next let  $g = \nabla L(x) - \frac{\langle \nabla L(x), x \rangle}{\|x\|^2} x$ . This is the orthogonalized gradient.
3. We update  $x' = x - \eta g$ .

Without renormalization, we are able to prove some desirable convergence properties. Not only that the algorithm converges under standard assumptions, but additionally the stable points have desirable properties when it comes to positive homogenous model architectures.

**Theorem 3.1** Suppose  $L : \mathbb{R}^n \rightarrow \mathbb{R}$  is bounded from below, differentiable, and  $\nabla L$  is Lipschitz with Lipschitz constant  $k$ . Then for any  $\eta \in (0, 1/k)$ , and any non-zero initialization  $x_0 \in \mathbb{R}^n$ ,  $\perp$ Grad (without gradient renormalization) will converge to some  $x^*$  satisfying:

$$|\langle \nabla L(x^*), x^* \rangle| = \|x^*\| \cdot \|\nabla L(x^*)\|.$$

In particular,  $\nabla L(x^*)$  is parallel to  $x^*$ .

*Proof.* Let  $x_k$  be any point along the  $\perp$ Grad pathway and let

$$g_k = \nabla L(x_k) - \langle \nabla L(x_k), x_k \rangle \frac{x_k}{\|x_k\|^2}$$

denote the orthogonalized gradient. Define the update  $x_{k+1} = x_k - \eta g_k$ . Since  $\nabla L$  is Lipschitz with constant  $k$ , we apply a standard descent bound:

$$\begin{aligned} L(x_{k+1}) &\leq L(x_k) - \eta \langle \nabla L(x_k), g_k \rangle + \frac{\eta^2 k}{2} \|g_k\|^2 \\ &= L(x_k) - \eta \left( \|\nabla L(x_k)\|^2 - \frac{\langle \nabla L(x_k), x_k \rangle^2}{\|x_k\|^2} \right) + \frac{\eta^2 k}{2} \|g_k\|^2 \\ &= L(x_k) - \eta \|g_k\|^2 + \frac{\eta^2 k}{2} \|g_k\|^2 \\ &= L(x_k) - \eta \left( 1 - \frac{\eta k}{2} \right) \|g_k\|^2. \end{aligned}$$

Since  $\eta < 1/k$ , the coefficient  $\eta \left( 1 - \frac{\eta k}{2} \right)$  is positive. Therefore, the loss strictly decreases unless  $g_k = 0$ . Summing over  $k = 0$  to  $T - 1$ , we get:

$$L(x_0) - L(x_T) \geq \eta \left( 1 - \frac{k\eta}{2} \right) \sum_{k=0}^{T-1} \|g_k\|^2.$$

Since  $L$  is bounded below by some  $L_{\inf} \in \mathbb{R}$ , we have:

$$\sum_{k=0}^{\infty} \|g_k\|^2 \leq \frac{L(x_0) - L_{\inf}}{\eta \left( 1 - \frac{k\eta}{2} \right)}.$$

We now note that since for each  $k \in \mathbb{N}$ ,  $\langle g_k, x_k \rangle = 0$ , we know

$$\sum_{k=0}^{\infty} \|x_{k+1} - x_k\|^2 = \eta^2 \sum_{k=0}^{\infty} \|g_k\|^2 < \infty$$

and by the Cauchy criterion it must be the case that the sequence  $(x_k)$  converges to some  $x^*$ .

We now let

$$g^* = \nabla L(x^*) - \langle \nabla L(x^*), x^* \rangle \frac{x^*}{\|x^*\|^2}$$

By continuity of  $\nabla L(\cdot)$  it is easy to see that  $g^* = 0$ , and the desired result follows immediately.  $\square$

We note here that when it comes to performing orthogonalization for a model with parameters  $\theta \in \mathbb{R}^p$ , the proof still holds if the orthogonalization is occurring on the entire parameter set at once, or at the level of a partition of  $\theta$  (in particular at the layer level). The conclusion will only differ in that each component of the stabilized gradient  $\nabla L(x^*)$  will be parallel to the corresponding component of the vector  $x^*$  and each component may differ by scalar multiples. For the purposes of understanding the stability of decision boundaries in classification models, this distinction makes no difference.

### 7.3 Decision Boundary Properties of Stable Points

In this section we prove that a stable point for non-renormalized  $\perp$ Grad exhibits favorable properties for positive homogenous models. We provide a proof in the case of an MLP with  $L$  layers and ReLU activation function, but the general principles can be applied to models that are positive homogenous with respect to the components with which  $\perp$ Grad has orthogonalized gradients.

**Theorem 7.4.** *For a ReLU MLP  $f$  with  $L$  layers and any  $c > 0$ , if we scale the model parameters of  $f$  by  $c$ , the decision boundary remains unchanged.*

*Proof.* Let  $f : \mathbb{R}^d \rightarrow \mathbb{R}^k$  represent the outputs of our neural network with  $L$  layers, i.e. for an input  $x$ ,  $f(x)$  represents the logits output by the model. We now let  $\tilde{f}$  represent the logits for the scaled model, where each weight and bias from  $f$  are multiplied by a factor of  $c$  for  $c > 0$ .

We will use induction to show that for every layer  $l$ , the hidden state  $\tilde{h}_l = c^l h_l$ . It will then directly follow that for all  $x$ ,  $\tilde{f}(x) = c^L f(x)$ . First assume that  $\tilde{h}_{l-1} = c^{l-1} h_{l-1}$ . Then we have:

$$\begin{aligned} \tilde{z}_l &= \tilde{W}_l \tilde{h}_{l-1} + \tilde{b}_l \\ &= c W_l ((1 + \epsilon)^{l-1} h_{l-1}) + c b_l \\ &= c^l W_l h_{l-1} + c b_l \\ &= c^l (W_l h_{l-1} + b_l) \\ &= c^l z_l \end{aligned}$$

We now apply ReLU (which is positively homogeneous):

$$\tilde{h}_l = \phi(\tilde{z}_l) = \phi(c^l z_l) = c^l \phi(z_l) = c^l h_l$$

So by induction:

$$f(x) = c^L h_L = \tilde{h}_L = \tilde{f}(x)$$

We now note that for any input value  $x \in \mathbb{R}^d$ , the predicted class is determined by the max logit of  $f(x)$ . By the above proof this max value is unchanged by scaling the model weights by  $c$  for any  $c > 0$ . We can therefore conclude that scaling the model weights and biases does not change the decision boundary, it only scales the model confidence (and when  $c > 1$  increases model confidence).  $\square$

### 7.4 Additional Figures

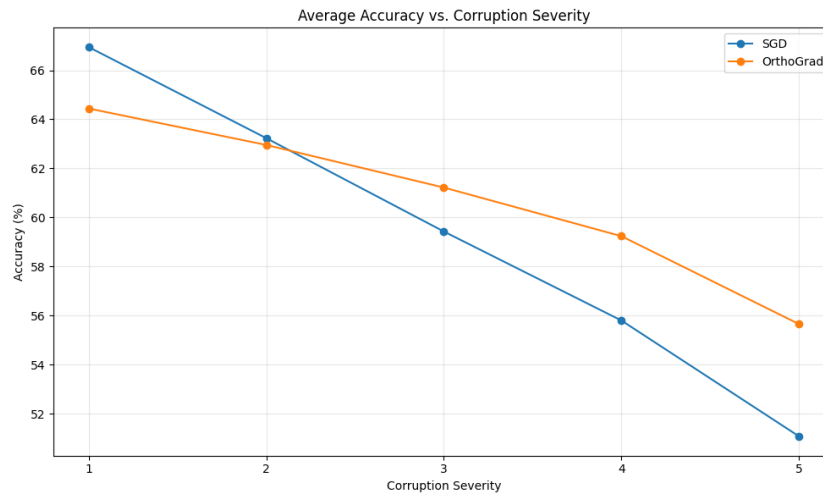


Figure 2: **Overtrained ResNet-18 accuracy across CIFAR-10C corruption levels.** In the over-trained environment accuracy initially favors SGD, however  $\perp$ Grad surpasses it at higher severity.

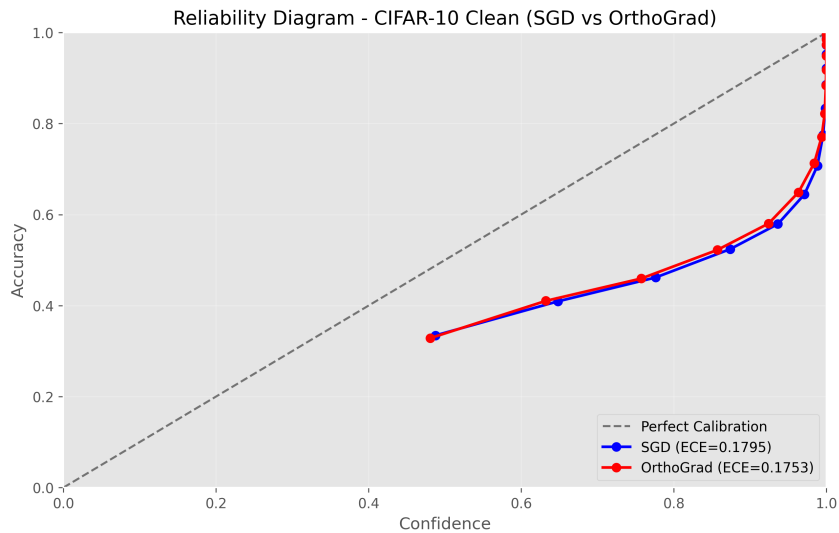


Figure 3: **Reliability Diagram for ResNet18 on CIFAR-10.** Average reliability diagram across 20 seeds across entire CIFAR-10 test dataset.  $\perp$ Grad exhibits slightly better reliability than SGD.

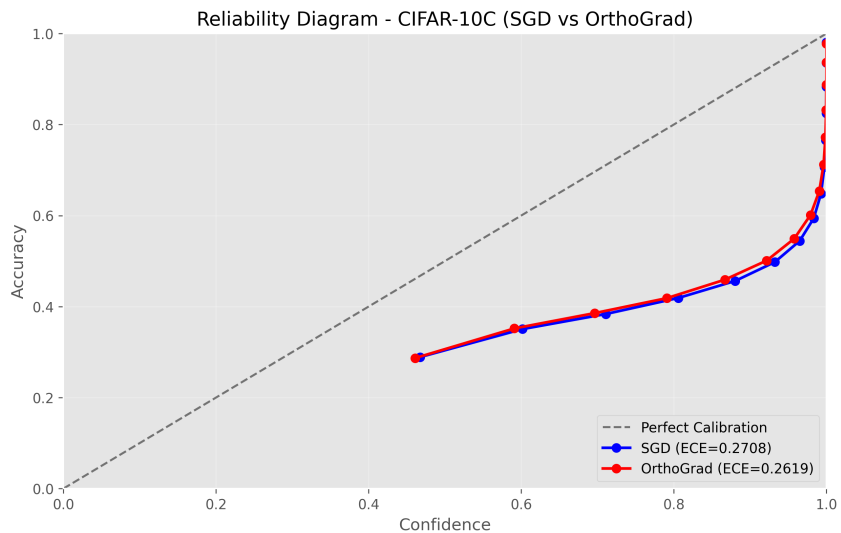


Figure 4: **Reliability Diagram for ResNet18 on CIFAR-10C.** Average reliability diagram across 20 seeds across entire CIFAR-10C test dataset.  $\perp$ Grad exhibits slightly better reliability than SGD.

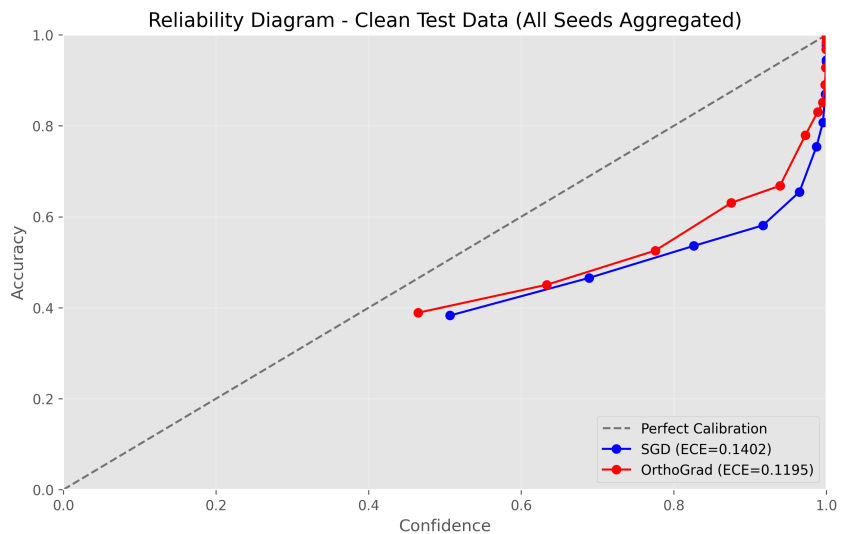


Figure 5: **Reliability Diagram for WideResNet-28-10 on CIFAR-10.** Average reliability diagram across 5 seeds.  $\perp$ Grad exhibits consistently better reliability than SGD.

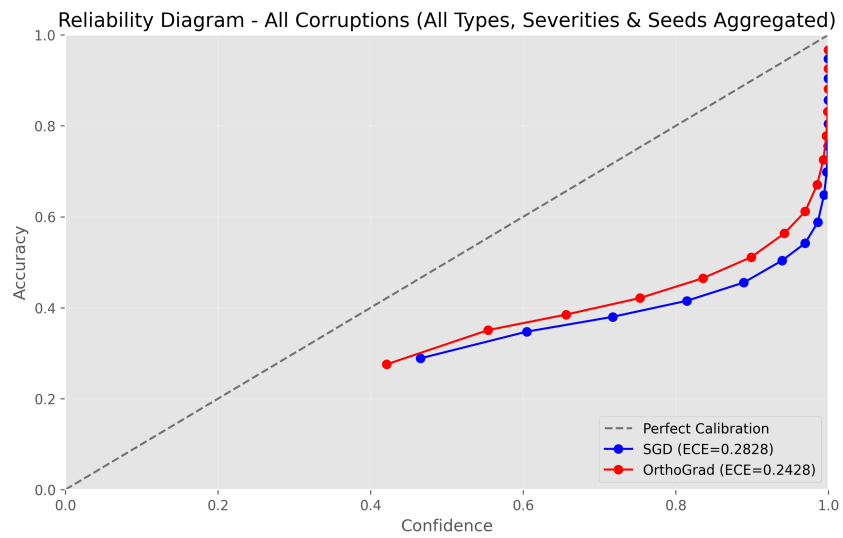


Figure 6: **Reliability Diagram for WideResNet-28-10 on CIFAR-10C.** Average reliability diagram across 5 seeds across entire CIFAR-10C test dataset.  $\perp$ Grad exhibits consistently better reliability than SGD.